Macromolecules

ARTICLE

pubs.acs.org/Macromolecules

# Nature of the Sub-Rouse Modes in the Glass−Rubber Transition Zone of Amorphous Polymers

Xuebang Wu,[†] Changsong Liu,[*,†] Zhengang Zhu,[†] K. L. Ngai,[*,‡,§] and Li-Min Wang[‡]

[†]Key Laboratory of Materials Physics, Institute of Solid State Physics, Chinese Academy of Sciences, P.O. Box1129, Hefei, Anhui, People's Republic of China

[‡]State Key Lab of Metastable Materials Science and Technology, and College of Materials Science and Engineering, Yanshan University, Qinhuangdao, Hebei, 066004, People's Republic of China

[§]CNR-IPCF Associate, Dipartimento di Fisica, Università di Pisa, Largo Bruno Pontecorvo 3, I-56127, Pisa, Italy

**ABSTRACT:** The shear mechanical compliance of the glass−rubber transition or softening zone of high molecular weight amorphous polymers typically increases from the glassy compliance of $\sim 10^{-10}$ cm$^2$/dyn up to the rubbery plateau of $\sim 10^{-6}$ cm$^2$/dyn. The contributions from the local segmental relaxation and the Rouse modes cannot account for the entire range of compliance, leaving three decades of compliance in between their contributions unaccounted for. Although new viscoelastic mechanism called sub-Rouse modes with length scales intermediate between the local segmental relaxation and the Rouse modes have been found to fill the void, so far they have not been found in archetypal polymers including polystyrene (PS) and poly(methyl methacrylate) (PMMA). This calls the generality of the existence of sub-Rouse modes into question. Using high precision shear mechanical spectroscopic tool, we report the observation of the sub-Rouse modes in PS and PMMA. From the various properties of the sub-Rouse modes determined, we find that the sub-Rouse modes are intermolecularly coupled like the local segmental relaxation, albeit to a less degree. The results are isomorphic to those found in poly(vinyl acetate) (PVAc) and PVAc−poly(ethylene oxide) (PVAc−PEO) blends. Thus, the sub-Rouse modes and its properties seem general in amorphous polymers.

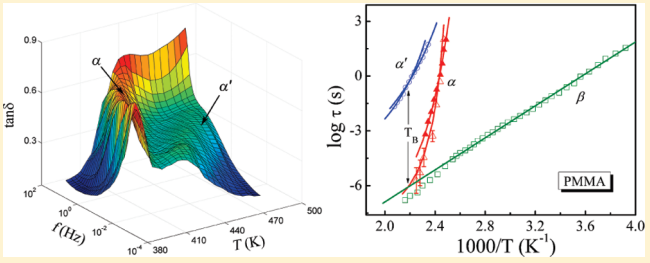


## I. INTRODUCTION

From the accumulated studies of by many researchers for more than half a century, the research field of polymer viscoelastic properties has arrived at a stage of becoming mature. Well established is the existence of essentially four zones of viscoelastic response of high molecular weight un-cross-linked and amorphous polymers.[1] These are (1) the glassy state, (2) the glass−rubber transition, also referred to as the softening transition/dispersion, (3) the rubbery plateau, and (4) the terminal zones, given here in order of increasing time scales of the viscoelastic response. Attempts have been made to relate viscoelastic response in each zone to molecular motions. In this paper, we limit our study and discussion on the glass−rubber transition zone. The fastest relaxation within this zone is the segmental relaxation which is responsible for the glass transition phenomenon and its enthalpic nature makes possible detection by calorimetry. Although the segmental relaxation requires cooperative motion from repeat units of different chains, the number of repeat units in each chain involved is small, and therefore it is more appropriate to call it the local segmental relaxation. This has been found from results of molecular dynamics simulations,[2] and NMR measurements of spin−lattice relaxation times indicating that the motions cover local segments up to three repeat units.[3] Also it can be inferred from creep compliance measurements of lower molecular weight polymers such as PS and PMPS with results described as follows. The creep compliance contributed by the segmental α-relaxation of polystyrene[4−6] and poly(methylphenylsiloxane)[7] are well fitted by the time dependence proposed by Read et al.,[8]

$$J_\alpha(t) = J_g + (J_{e\alpha} - J_g)[1 - \exp(-(t/\tau_\alpha)^{1-n_\alpha}] \quad (1)$$

where $0 < (1 - n_\alpha) \equiv \beta_\alpha \leq 1$. The size of the difference, $(J_{e\alpha} - J_g)$, of the polymers at the glass transition temperature $T_g$ is about the same as that found for small molecular glassformers such as *o*-terphenyl and trinaphthalbenzene.[9] Most importantly, $J_{e\alpha}$ is only about four or five times larger than $J_g$ in PS[4−6] and PMPS,[7] comparable to that found in trinaphthalbenzene. However the compliance in glass−rubber transition zone of entangled polymers starts from the glassy compliance $J_g$, typically of the order of $10^{-10}$ cm$^2$/dyn, and rises 4 orders of magnitude to the plateau compliance of about $10^{-6}$ cm$^2$/dyn. Thus, there is need to account for the other molecular mechanisms contributing to compliance within the glass−rubber transition zone from $J_{e\alpha} \approx 5 \times 10^{-10}$ to $10^{-6}$ cm$^2$/dyn. Another way to see the need is

**Received:** December 21, 2010
**Revised:** February 20, 2011
**Published:** April 05, 2011

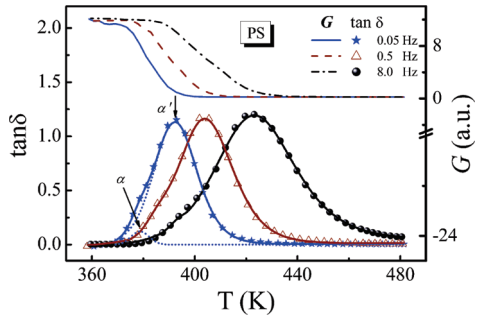


**Figure 1.** Temperature-dependent mechanical relaxation spectra (tan $\delta$ and $G$) of PS at 0.05, 0.5, and 8.0 Hz. Dotted lines are the fits of the α and α′ peaks using a nonlinear fitting method.

by length-scale consideration. The glass−rubber transition zone encompasses all the viscoelastic mechanisms with length scales in between the glassy zone and the rubbery plateau region. The onset of the plateau is determined by the entanglement molecular weight, which for PS is 16 000 or 160 repeat units. Thus, there are relaxation mechanisms having length scales longer than a few repeat units for local segmental relaxation and up to the upper limit of a few hundred repeat units. Traditionally, the relaxation modes from the bead−spring model of Rouse generalized to undiluted polymers[1] have been considered solely such relaxation mechanisms in the glass−rubber transition zone. Notwithstanding common acceptance of this proposition, M. L. Williams had shown long ago[10] that the Rouse modes can only account for compliance in the glass−rubber transition zone of the order of magnitude larger than the lower bound of $10^{-8}$ cm$^2$/dyn. This estimate from Williams was obtained for PS with molecular weight 150 000 g/mol and a density of 1.5 g/cm$^3$ and assuming that the smallest submolecule that can be still be Gaussian in the Rouse model consists of five repeat units. Increasing the number of repeat units than five for the Gaussian submolecule would make the lower bound even larger than $10^{-8}$ cm$^2$/dyn. Thus, the extended Rouse model cannot account entirely the void in the glass−rubber transition of entangled polymers, and another kind of relaxation mechanism must be present which has longer (shorter) length scale and relaxation times than the local segmental relaxation (the Rouse modes). Naturally they were referred to as sub-Rouse modes. For the first time, sub-Rouse modes were found together with the local segmental relaxation by photon correlation spectroscopy,[11,12] and together with the Rouse modes by creep compliance and dynamic mechanical relaxation[13] in polyisobutylene (PIB). This polymer was chosen because it has a very broad glass−rubber transition zone, which makes it easier to resolve the sub-Rouse modes from the local segmental relaxation and the Rouse modes. The temperature dependence of the relaxation times of the sub-Rouse modes, $\tau_{sR}$, in PIB is weaker than that of the local segmental α-relaxation time, $\tau_\alpha$, but stronger than that of the Rouse relaxation time, $\tau_R$. The temperature dependence of $\tau_{sR}$ together with its difference from those of $\tau_\alpha$ and $\tau_R$ was exploited to deduce that the sub-Rouse modes are also intermolecularly coupled or cooperative like the local segmental relaxation albeit to a lesser degree.[12] This is a deduction, and direct experimental evidence is much needed to know more about the nature of the sub-Rouse modes.

Since the discovery of the existence of the sub-Rouse modes in PIB 15 years ago by light scattering, creep compliance, and dynamic modulus measurements, no serious attempts to look for sub-Rouse modes in other polymers have been reported until very recently. One is the successful detection of sub-Rouse modes by dielectric spectroscopy in polyisoprene (PIP), head-to-head polypropylene (hhPP), and also in the same sample of PIB used earlier to detect sub-Rouse modes by dielectric measurements.[14] Although nice to have confirmation of the existence of sub-Rouse modes in PIB and two more polymers by the dielectric relaxation, the results have not shed more light on the nature of the sub-Rouse modes. Besides, it was pointed out by the authors of ref[14] that dielectric spectroscopy has limitation and cannot detect sub-Rouse modes of many polymers. The most notable polymers missing are polystyrene (PS) and atactic polypropylene (aPP). This is a pity because PS is often considered as the standard of all amorphous polymers and is the most studied amorphous polymers by mechanical spectroscopy of various kinds,[1] nuclear magnetic resonance,[15,16] and photon correlation spectroscopy.[17] Thus, it has become a pressing issue to look for sub-Rouse modes in PS. The situation is the same in the case of poly(methyl methacrylate) (PMMA).[1,18,19]

One purpose of this study is to look for sub-Rouse modes in PS by high precision low-frequency mechanical spectroscopy.[20] It was found, and moreover its properties indicate that the sub-Rouse modes in PS are intermolecularly coupled and cooperative like local segmental α-relaxation, although to a lesser degree. Another purpose of the paper is to show these properties of sub-Rouse modes in PS are general for polymers by presenting currently unpublished data of PMMA and by bringing back for discussion previously published data of PVAc and PEO/PVAc blends.

## II. EXPERIMENTAL SECTION

The samples are polystyrene with molecular weight $M_w$ = 21 kg/mol and $M_w/M_n$ = 1.04, and PMMA with $M_w$ = 120 kg/mol and $M_w/M_n$ = 1.8. Measurements of shear mechanical loss of the two samples were made by using a modified low-frequency inverted torsion pendulum with a Couette-like setup using the forced-vibration method. Details of the setup and the procedure of acquiring data have been presented before in refs.[20−22] The isothermal loss tangent (tan $\delta$) and the relative shear modulus $G$ were measured over a frequency range from $5 \times 10^{-3}$ to 100 Hz at constant temperatures. These isothermal measurements were first carried out at some low temperature and thereafter at higher temperatures incremented by small steps. Isochronal measurements of tan $\delta$ and $G$ were also made over a temperature range 360−480 K for PS and 360−550 K for PMMA at fixed frequencies of 0.05, 0.5, and 8.0 Hz.

## III. RESULTS AND DISCUSSION

The loss tangent, tan $\delta$, is an alternative to the storage modulus $G'$ and loss modulus $G''$ to characterize the viscoelastic properties of polymers. For some viscoelastic mechanisms, tan $\delta$ is more prominent and sensitive to changes in temperature in isochronal measurement and in frequency in isothermal measurements than $G'$ and $G''$. This is the case for modes of relaxation involving motion of longer scales such as the sub-Rouse modes and Rouse modes. On the other hand, the local segmental or the α-relaxation shows up more favorably as loss peaks when mechanical data are presented by $G''$.[4,23] The mechanical spectra given in terms of tan $\delta$ and $G$ of PS and PMMA at several frequencies are shown in the temperature ranges of 360−480 K and 360−550 K in Figures 1 and 2 respectively. The mechanical loss exhibits an asymmetrical broad peak with a shoulder at the

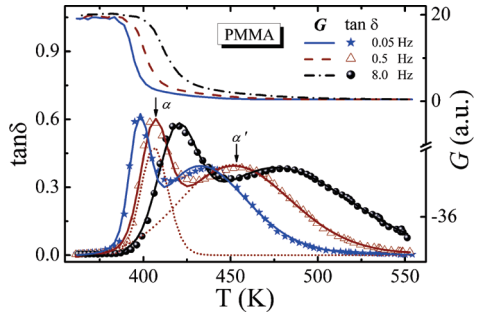


**Figure 2.** Temperature-dependent mechanical relaxation spectra (tan $\delta$ and $G$) of PMMA at 0.05, 0.5, and 8.0 Hz. Dotted lines are the fits of the α and α′ peaks using a nonlinear fitting method.

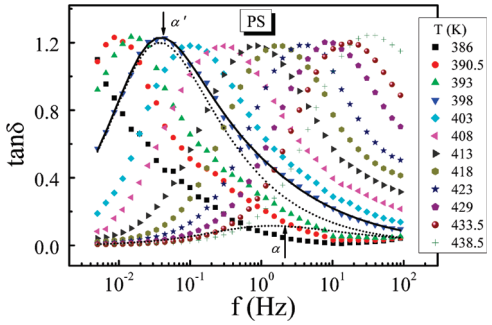


**Figure 3.** Isothermal mechanical loss tangent spectra of PS at different temperatures. Dotted lines are the fitting of the tan $\delta$ peak at 398 K.

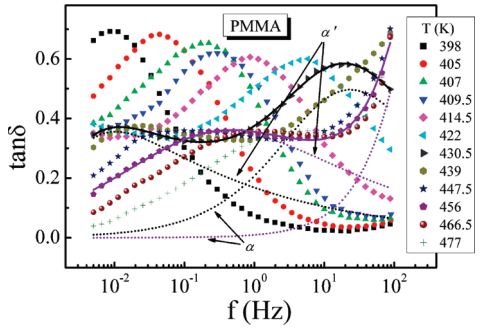


**Figure 4.** Isothermal mechanical loss tangent spectra of PMMA at different temperatures. Dotted lines are the fits of the tan $\delta$ peak at 430.5 and 456 K.

low temperature side for PS, but two resolved loss peaks for PMMA. The asymmetrical structure of PS could be fitted by loss peaks from two processes, α and α′ peaks, with distributions in relaxation time using a nonlinear fitting method.[24,25] The two loss peaks from α and α′ processes obtained from the fits of the data of PS at 0.05 Hz and PMMA at 0.5 Hz are shown in Figures 1 and 2 respectively. Note that the mechanical relaxation of PMMA with the similar $M_w$ have been measured previously by Pakula but his tan $\delta$ data do not exhibit the α′ peak.[26] The reason why Pakula did not observe the α′ peak is because the highest temperature reached by him was about 485 K, which is not sufficient to see the α′ peak occurring at higher temperatures. By using a improved mechanical relaxation equipment, we can go up in temperature as high as 550 K and the α′ peak is clearly

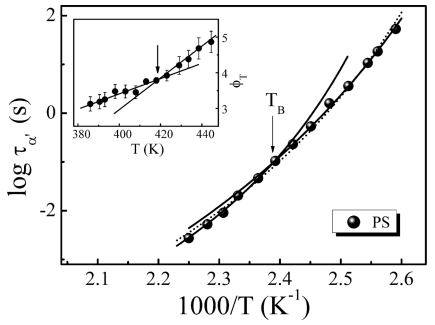


**Figure 5.** Temperature dependence of relaxation time of α′ mode for PS. The solid lines represent the two VFTs for the polymers and a crossover is clearly seen. The dotted line corresponds to the fitting by a single VFT equation and the parameters are as follows: log $\tau_0 = -8.1$, $D = 5.6$, and $T_0 = 310$ K. The inset shows the plots of the Stickel function, $\phi_T = (-\mathrm{d}[\log(\tau_{\alpha'}(T))]/\mathrm{d}T)^{-1/2}$, against temperature. The crossover temperature, $T_B \sim 417$ K, has been estimated by the intersection of two straight lines.

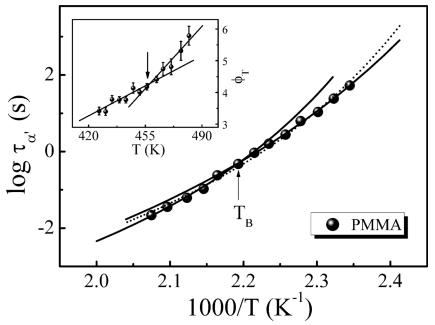


**Figure 6.** Temperature dependence of relaxation time of α′ mode for PMMA. The solid lines represent the two VFTs for the polymers and a crossover is clearly seen. The dotted line corresponds to the fitting by a single VFT equation and the parameters are as follows: log $\tau_0 = -6.6$, $D = 4.6$, and $T_0 = 345$ K. The inset shows the plots of the Stickel function, $\phi_T = (-\mathrm{d}[\log(\tau_{\alpha'}(T))]/\mathrm{d}T)^{-1/2}$, against temperature. The crossover temperature, $T_B \sim 454$ K, has been estimated by the intersection of two straight lines.

observed. The loss peak α at lower temperature is associated with the faster relaxation. This is particularly clear for PMMA where the lower temperature loss peak is located approximately at $T_g$ determined by DSC measurements. Naturally the slower α′-process is associated with motion of more repeat units in each chain than the α-process.

The isothermal mechanical loss tangent spectra of PS and PMMA are shown in Figures 3 and 4, respectively, at different temperatures above $T_g$. The tan $\delta$ peak of PS at any temperature in these figures is associated with the α′-process and the α-process appearing at higher frequencies contributes little and is not completely resolved at higher temperatures. For PMMA, the tan $\delta$ peak at lower frequencies originates from the α′-process, while the tan $\delta$ peak at higher frequencies comes from the α-process. To obtain the relaxation time and frequency dispersion of the two processes, the spectra are fitted by additive contributions of two Havriliak−Negami (HN) functions for tan $\delta$ according to,

$$\tan\delta = \sum_{i=1,2} \Delta_i / [1 + (i\omega\tau_i)^{\lambda_i}]^{\gamma_i} \qquad (2)$$


dx.doi.org/10.1021/ma102897e |Macromolecules 2011, 44, 3605–3610

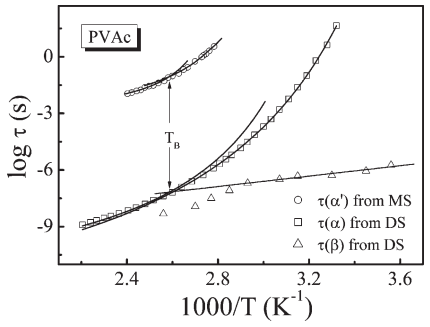


**Figure 7.** Temperature variations of characteristic relaxation times of PVAc for mechanical α′ (○) relaxation, and dielectric α (□) and $\beta$ (Δ) relaxations (ref 29). Data of $\beta$ relaxation are fitted by Arrhenius law, while data of the α and α′ relaxations are fitted by two VFT equations. Nearly the same crossover temperature $T_B$ for both the α and α′ relaxations is demonstrated by the vertical arrows.

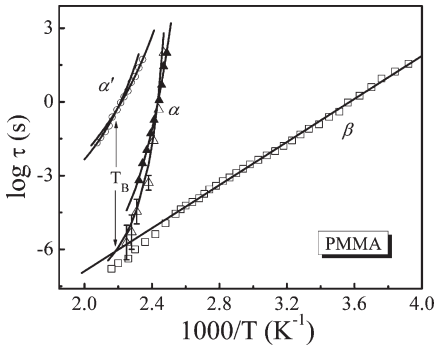


**Figure 8.** Temperature dependences of characteristic relaxation times of PMMA for mechanical α (▲) and α′ (○) relaxations, and dielectric α (Δ) and $\beta$ (□) relaxations (ref 30). The $\beta$ relaxation are fitted by Arrhenius law, and the α relaxations are fitted by a single VFT equation, while the α′ relaxation is fitted by two VFT equations.

where $\Delta_i$ is the relaxation strength, and $\lambda_i$ and $\gamma_i$ are fractions of unity. From the fits, the relaxation time, $\tau_{\alpha'}$ and the frequency dispersion of the α′-process are obtained as a function of temperature for PS and PMMA. As an example, the two HN functions that fit the α′-process and α-process of PS at 398 K are shown in Figure 3. For PMMA, the well resolved α′-process and α-process enable $\tau_{\alpha'}$ to be determined accurately even at temperatures above 439 K where the α-process cannot be captured in its entirety. Two examples of the fits to the spectra at 430.5 and 456 K are shown in Figure 4.

In Figures 5 and 6, we plot the temperature dependence of characteristic relaxation time $\tau_{\alpha'}$ of α′-process of PS and PMMA respectively. Normally, the temperature dependence of relaxation time could be described by the Vogel−Fulcher−Tammann (VFT) equation.

$$\tau(T) = \tau_0 \exp\left(\frac{DT_0}{T - T_0}\right) \qquad (3)$$

where $T_0$, the Vogel temperature, $D$ and $\tau_0$ are material dependent constants. However, over the wide temperature range of the experiment, we find that the $\tau_{\alpha'}(T)$ dependence cannot be described satisfactorily by a single VFT equation, as shown by dotted lines in Figures 5 and 6. Two VFT equations are required to fit the data of PS and PMMA. The parameters of these VFT equations are given as follows. For PS, in the low-$T$ range, log $\tau_0$ = −8.8, $D$ = 7.6, and $T_0$ = 295 K, while in high-$T$ range, log $\tau_0$ = −7.2, $D$ = 3.3, and $T_0$ = 340 K; for PMMA, in low-$T$ range, log $\tau_0$ = −6.8, $D$ = 5.6, and $T_0$ = 332 K, while in high-$T$ range, log $\tau_0$ = −6.5, $D$ = 3.8, and $T_0$ = 361 K. For PMMA, this finding is not new, and it has been found in a lower molecular weight sample.[27] The change of $T$-dependence of $\tau_{\alpha'}(T)$ from one VFT law to another is confirmed by using the method proposed by Stickel and co-workers,[28] whereby the data $\tau_{\alpha'}(T)$ are transformed into $\phi_T = (-\mathrm{d}[\log(\tau_{\alpha'}(T))]/\mathrm{d}T)^{-1/2}$ as a function of $T$. The crossover of $\tau_{\alpha'}(T)$ in PS and PMMA from one VFT law to another is proven by the fact that $\phi_T$ exhibits a change in slope at some characteristic temperature $T_B$ (see insets of Figures 5 and 6). The crossover relaxation time $\tau_{\alpha'}(T_B)$ is about the same for PS and PMMA, and for PVAc and PVAc/PEO blends all with $\tau_{\alpha'}(T_B) \approx 10^{-1\pm0.5}$ s, apparently not sensitive to molecular structures. At this juncture, it is worthwhile to bring back for discussion the data of crossover of $T$-dependence of $\tau_{\alpha'}(T)$ in PVAc from similar mechanical relaxation measurements.[20] Not published before is

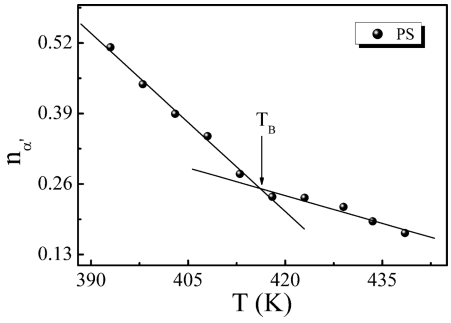


**Figure 9.** Temperature dependence of coupling parameter $n_{\alpha'}(T)$ for PS. The crossover temperature $T_B$ was marked by the change in temperature dependence of $n_{\alpha'}(T)$. The solid lines are guides to the eye.

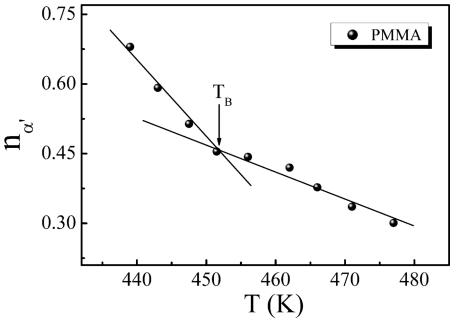


**Figure 10.** Temperature dependence of coupling parameter $n_{\alpha'}(T)$ for PMMA. The crossover temperature $T_B$ was marked by the change in temperature dependence of $n_{\alpha'}(T)$. The solid lines are guides to the eye.

the quantitative comparison between this crossover of $\tau_{\alpha'}(T)$ and a similar crossover of $\tau_\alpha(T)$ found by dielectric relaxation,[29] both experiments were performed on high molecular weight entangled PVAc. Such a comparison is made in Figure 7, where the crossover of $\tau_{\alpha'}(T)$ and the crossover of $\tau_\alpha(T)$ appear to occur at approximately the same temperature $T_B$. There is absence of mechanical or dielectric data for the α-process of PS and PMMA to show the crossover of $\tau_\alpha(T)$ at $T_B$. Empirically, $T_B$ for $\tau_\alpha(T)$ is found to be close to the temperature $T_\beta$ at the intersection of $\tau_\alpha(T)$ with the extrapolated Arrhenius $T$-dependence of the $\beta$-relaxation time, $\tau_\beta$, determined at temperatures

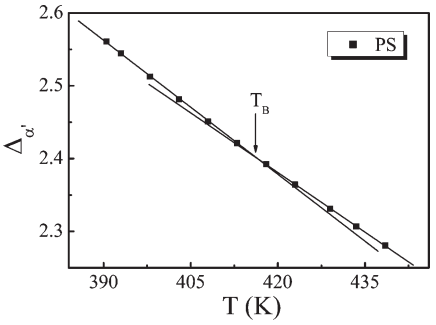


**Figure 11.** Temperature dependence of relaxation strength $\Delta_{\alpha'}$ of the $\alpha'$ mode for PS. The solid lines are guides to the eye and the crossover is clearly seen.

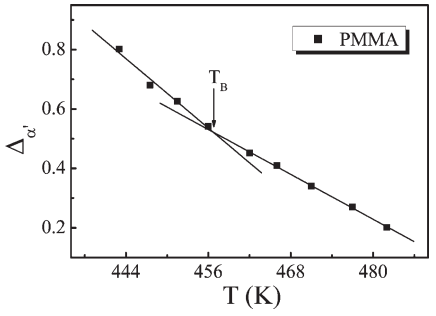


**Figure 12.** Temperature dependence of relaxation strength $\Delta_{\alpha'}$ of the $\alpha'$ mode for PMMA. The solid lines are guides to the eye and the crossover is clearly seen.

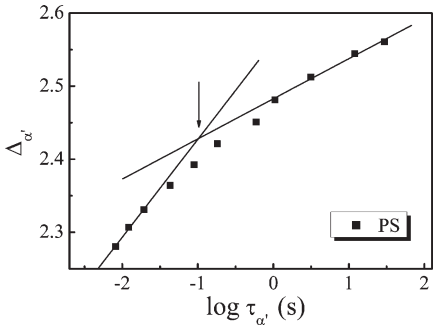


**Figure 13.** Variation of the relaxation strength $\Delta_{\alpha'}$ of the $\alpha'$ mode for PS as a function of the logarithm of the characteristic relaxation times. The change in slope reveals the crossover of $\Delta_{\alpha'}$ at $T_B$.

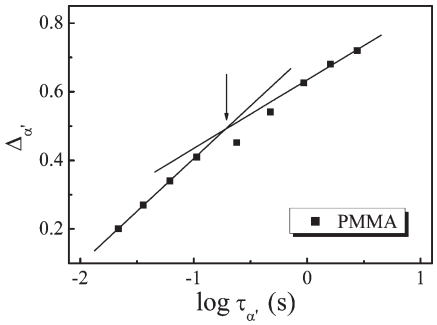


**Figure 14.** Variation of the relaxation strength $\Delta_{\alpha'}$ of the $\alpha'$ mode for PMMA as a function of the logarithm of the characteristic relaxation times. The change in slope reveals the crossover of $\Delta_{\alpha'}$ at $T_B$.

below $T_g$ to above $T_g$. In Figure 8 is shown the $T$-dependent relaxation time of the $\alpha'$-process and the $\alpha$-process for PMMA. Also included in the figure are literature results from dielectric measurements of Bergman et al.[30] The extrapolation performed for PMMA in Figure 8 demonstrates and $T_\beta$ so determined is in approximate agreement with the crossover temperature $T_B$ of $\tau_{\alpha'}(T)$. Thus, there is remarkable coincidence between the crossover temperatures of $\tau_{\alpha'}(T)$ and $\tau_\alpha(T)$. This does not happen by accident because of the presence of other analogous properties of the two kinds of crossover. These include the change of the $T$-dependence of the width of the dispersion from weaker one for $T > T_B$ to a stronger one for $T < T_B$ found for the $\alpha'$-process in ref 22 and for the $\alpha$-process in ref 29. This feature of the $\alpha'$-process is found in PS and PMMA as shown in Figures 9 and 10 respectively by plotting $n_{\alpha'}$ versus $T$, where $n_{\alpha'}$ appear in the exponent of the Kohlrausch-William-Watts (KWW) function,

$$\phi(t) = \exp[-(t/\tau)^{1-n}] \quad (4)$$

and $n$ is related to $w$, the full-width at half-maximum of the $\alpha'$-loss peak normalized by that of the Debye relaxation, by the relation $n = 1.041(1 - w^{-1})$.[29,31] Another analogous feature found in the two kinds of crossover is the change of the relaxation strength from a weaker $T$-dependence above $T_B$ to a stronger one below $T_B$, both are increasing with decreasing temperature as the Curie law suggests.[22,29]

The crossover of the $\alpha'$-process of PS and PMMA also can be reflected by the variation of relaxation strength $\Delta_{\alpha'}$. The dynamic crossover of $\Delta_{\alpha'}$ is clearly shown for both PS and PMMA in Figures 11 and 12. Note that above $T_B$, $\Delta_{\alpha'}$ decreases slowly with increasing temperature. This $T$-dependence of $\Delta_{\alpha'}$ is indicative of a cooperative relaxation decreasing in degree of cooperativity or length-scale due to enhanced thermal energy on increasing temperature.[32,33] Thus, the change in $\Delta_{\alpha'}$ with temperature can be used to show that the corresponding change in the extent of cooperativity of $\alpha'$ relaxation. The observation of decrease of $\Delta_{\alpha'}$ suggests that the extent of cooperativity of $\alpha'$-process decreases with increasing temperature, similar to the behavior of local segmental relaxation and structural $\alpha$-relaxation of glass-formers in general.

The relaxation strength $\Delta_{\alpha'}$ and the relaxation time $\tau_{\alpha'}$ reflect different and yet complementary properties of the same underlying relaxation process, and hence both should be correlated in their temperature dependence.[34] In Figures 13 and 14 we have plotted the relaxation strength of PS and PMMA against log $\tau_{\alpha'}$ in searching of such correlations. The plot can be separated into two regions, where $\Delta_{\alpha'}$ as a function of log $\tau_{\alpha'}$ can be described by two straight lines with different slopes. The intersection of two lines leads to a crossover relaxation time of nearly $10^{-1}$ s which corresponds to $\tau_0(T_B)$ of $\alpha'$-process obtained from the VFT analysis. It is apparent that $\Delta_{\alpha'}$ increases as a function of log $\tau_{\alpha'}$ much more rapidly in the regime $T > T_B$ than for $T < T_B$, consistent with the crossover at $T_B$ in Figures 5 and 6.

Plazek and co-workers found in PIB[12,13] that the $T$-dependence of the relaxation time of the sub-Rouse modes is weaker than that of the local segmental $\alpha$-relaxation, but stronger than that of the Rouse modes. Moreover, the length scale of the sub-Rouse modes naturally is intermediate in size between the Rouse modes and the $\alpha$-relaxation. Well known are the facts that the

Rouse modes is totally entropic and noncooperative, and the α-relaxation is cooperative. From its intermediate character seen by experiments in previous works, the sub-Rouse mode had been concluded to be cooperative but to a lesser degree than the α-process. Also there is support of this conclusion from the coupling model.[12,35] For PIB, the coupling parameter of the local segmental relaxation is larger than that for the sub-Rouse modes, while the coupling parameter of the Rouse modes is identically zero.[12] These previous works all have concluded that the α′-process is intermolecularly coupled and cooperative like the α-process, although to a lesser degree. This conclusion is strengthened by the principal result of the current study, which is the presence of crossover of dynamics in both the α′-process and the α-process at nearly the same temperature $T_B$ with similar change of associated properties in the crossing. Furthermore, the phenomenon of change in dynamics of the α′-process when crossing $T_B$ are shared by different polymers, indicating that the sub-Rouse modes and their properties are universal. Since the Rouse modes are entropic and noncooperative, they have to be distinguished from the α′-process that we have observed. The α′-process are relaxation mechanism with time scale and length scale intermediate between the local segmental relaxation (α-process) and the Rouse modes. Thus, the terminology, sub-Rouse modes, given to them is appropriate.

## IV. CONCLUSIONS

Sub-Rouse modes are found in the archetypal amorphous polymers PS and PMMA by precision mechanical relaxation spectroscopy. They exhibit properties similar to those of local segmental relaxation. These similar properties indicate that the sub-Rouse modes, like the local segmental relaxation, are intermolecularly coupled and their dynamics are cooperative. The results here are identical to those of sub-Rouse modes found recently in PVAc and PVAc−PEO blends. Hence we conclude the existence of the sub-Rouse modes in the glass−rubber transition zone of amorphous polymers, as well as their properties and characteristics are universal. The part of the conclusion on the universal presence of the sub-Rouse modes in amorphous polymers is reinforced by the observations of sub-Rouse modes in different polymers by other workers. These additional observations of sub-Rouse modes in polymers include polyisobutylene (PIB) and butyl rubber, by shear compliance and modulus,[13,23,36] and PIB, polyisoprene (PIP) and head-to-head polypropylene[14] and natural rubber,[23] by dielectric relaxation. It is worthwhile to emphasize that characterization of the sub-Rouse modes was not made in the previous works by others to reveal the cooperative nature of the dynamics, like we have done in this paper.

## AUTHOR INFORMATION

### Corresponding Author

*E-mail: (C.L.) csliu@issp.ac.cn; (K.L.N.) ngai@df.unipi.it.

## ACKNOWLEDGMENT

This work at Key Laboratory of Materials Physics, Institute of Solid State Physics, Chinese Academy of Sciences was financially supported by National Natural Science Foundation of China (50803066, 10874182, and 11074253). At Yanshan University, it was supported by National Basic Research Program of China (973 Program No. 2010CB731604), and by NSFC (Grant Nos. 50731005, 50821001, 10804093, and 51071138).

## REFERENCES

(1) Ferry, J. D. *Viscoelastic Properties of Polymers*, 3rd ed.; John Wiley: New York, 1980.
(2) Adolf, D. B.; Ediger, M. D. *Macromolecules* **1992**, *25*, 1074.
(3) Krajewski-Bertrand, M. A.; Laupretre, F. *Macromolecules* **1996**, *29*, 7616.
(4) Ngai, K. L.; Plazek, D. J. *Rubber Chem. Technol. Rubber Rev.* **1995**, *68*, 376.
(5) Plazek, D. J.; O'Rourke, V. M. *J. Polym. Sci., Part A-2: Polym. Phys.* **1971**, *9*, 209.
(6) Ngai, K. L.; Plazek, D. J.; Echeverria, I. *Macromolecules* **1996**, *29*, 7937.
(7) Plazek, D. J.; Bero, C.; Neumeister, S.; Floudas, G.; Fytas, G.; Ngai, K. L. *Colloid Polym. Sci.* **1994**, *272*, 1430.
(8) Read, B. E.; Tomlins, P. E.; Dean, G. D. *Polymer* **1990**, *31*, 1204.
(9) Plazek, D. J.; Magill, J. H. *J. Chem. Phys.* **1996**, *45*, 3038.
(10) Williams, M. L. *J. Polym. Sci.* **1962**, *62*, 57.
(11) Rizos, A. K.; Jian, T.; Ngai, K. L. *Macromolecules* **1995**, *28*, 517.
(12) Ngai, K. L.; Plazek, D. J.; Rizos, A. K. *J. Polym. Sci., Part B: Polym. Phys.* **1997**, *35*, 599.
(13) Plazek, D. J.; Chay, I. C.; Ngai, K. L.; Roland, C. M. *Macromolecules* **1995**, *28*, 6432.
(14) Paluch, M.; Pawlus, S.; Sokolov, A. P.; Ngai, K. L. *Macromolecules* **2010**, *43*, 3103.
(15) Spiess, H. W. *J. Non-Cryst. Solids* **1991**, *131−133*, 766.
(16) Kaufmann, S.; Wefing, S.; Schaefer, D.; Spiess, H. W. *J. Chem. Phys.* **1990**, *93*, 197.
(17) Lindsey, C. P.; Pattersn, G. D.; Stevens, J. R. *J. Polym. Sci., Part B: Polym. Phys.* **1979**, *17*, 1547.
(18) Schmidt-Rohr, K.; Kulik, A. S.; Beckham, H. W.; Ohlemacher, A.; Pawelzik, U.; Boeffel, C.; Spiess, H. W. *Macromolecules* **1994**, *27*, 4733.
(19) Kulik, A. S.; Beckham, H. W.; Schmidt-Rohr, K.; Radloff, D.; Pawelzik, U.; Boeffel, C.; Spiess, H. W. *Macromolecules* **1994**, *27*, 4746.
(20) Wu, X. B.; Zhu, Z. G. *J. Phys. Chem. B* **2009**, *113*, 11147.
(21) Wu, X. B.; Xu, Q. L.; Shui, J. P.; Zhu, Z. G. *Rev. Sci. Instrum.* **2008**, *79*, 126105.
(22) Wu, X. B.; Wang, H. G.; Liu, C. S.; Zhu, Z. G. *Soft Matter* **2011**, *7*, 579.
(23) Donth, E.; Beiner, M.; Reissig, S.; Korus, J.; Garwe, F.; Vieweg, S.; Kahle, S.; Hempel, E.; Schröter, K. *Macromolecules* **1996**, *29*, 6589.
(24) Yuan, L. X.; Fang, Q. F. *Acta Met. Sinica* **1998**, *34*, 1016.
(25) Wang, X. P.; Fang, Q. F. *J. Phys.: Condens. Matter* **2001**, *13*, 1641.
(26) Kremer, F.; Schönhal, A., Eds. *Broadband Dielectric Spectroscopy*; Springer: Berlin, 2003; p 609.
(27) Wu, X. B.; Zhou, X. M.; Liu, C. S.; Zhu, Z. G. *J. Appl. Phys.* **2009**, *106*, 013527.
(28) Stickel, F.; Fischer, E. W.; Richert, R. *J. Chem. Phys.* **1995**, *102*, 6251.
(29) Ngai, K. L.; Roland, C. M. *Polymer* **2002**, *43*, 567.
(30) Bergman, R.; Alvarez, F.; Alegría, A.; Colmenero, J. *J. Chem. Phys.* **1998**, *109*, 7546.
(31) Dixon, P. K. *Phys. Rev. B* **1990**, *42*, 8179.
(32) Jin, X.; Zhang, S. H.; Runt, J. *Macromolecules* **2003**, *36*, 8033.
(33) Schönhals, A. In *Dielectric Spectroscopy of Polymer Materials: Fundamentals and Applications*; Runt, J. P., Fitzgerald, J. J., Eds.; American Chemical Society: Washington, DC, 1997; p 107.
(34) Schönhals, A. *Europhys. Lett.* **2001**, *56*, 815.
(35) Ngai, K. L.; Plazek, D. J.; Rendell, R. W. *Rheol. Acta* **1997**, *36*, 307.
(36) Kilburn, D.; Wawryszczuk, J.; Dlubek, G.; Pionteck, J.; Hässler, R.; Alam, M. A. *Macromol. Chem. Phys.* **2006**, *207*, 721.